Available online at www.sciencedirect.com
ScienceDirect
Journal of the European Ceramic Society 29 (2009) 2635–2641
www.elsevier.com/locate/jeurceramsoc

# Effect of temperature on the pre-creep mechanical properties of silicon nitride

Estíbaliz Sánchez-González *, Pedro Miranda, Fernando Guiberteau, Antonia Pajares

*Departamento de Ingeniería Mecánica, Energética y de los Materiales, Escuela de Ingenierías Industriales, Universidad de Extremadura, 06071 Badajoz, Spain*

Received 16 December 2008; received in revised form 10 March 2009; accepted 16 March 2009
Available online 15 April 2009

**Abstract**

The elasto-plastic properties and contact damage evolution of a commercial polycrystalline silicon nitride are evaluated as a function of temperature up to 1000 °C, using a recently developed method combining Hertzian indentation and FEM simulation. The results of the study are compared to existing data for other ceramic materials such as alumina and zirconia. Silicon nitride is found to exhibit an excellent combination of elasto-plastic properties in the pre-creep temperature range and good contact damage resistance. These qualities make this material ideal for high temperature applications in general, and in particular to be used in spherical indenters for the evaluation of mechanical properties of other materials at elevated temperature using the procedure applied in this work.


*Keywords:* Hertzian test; Silicon nitride; Mechanical properties; Contact fracture; Temperature dependence

## 1. Introduction

In previous work a new method for evaluating the mechanical properties of ceramic materials above room temperature was developed.[1] The technique is based on Hertzian indentation tests combined with finite element modeling (FEM), and allows one to obtain the elasto-plastic properties — Young's modulus, quasi-plastic yield stress and strain-hardening parameter — of the tested materials. The method has so far been applied to study the effect of temperature on the mechanical properties of zirconia Y–PSZ[2] and alumina[3] using spherical indenters of zirconia and alumina, respectively. Since it is difficult to machine spheres from every material of interest, and in order to standardize the procedure, it is necessary to select the most suitable material for the spherical indenter. Considering that the range of materials commercially available as precision spheres is limited, and that tungsten carbide, the most commonly used indenter material at room temperature, is unsuitable above 500 °C in air, silicon nitride ($Si_3N_4$) appears to be an appealing candidate for this task.

Silicon nitride is today playing a major role as a technological ceramic due to its excellent combination of properties—high toughness, good strength even at high temperatures, outstanding thermal shock resistance, remarkable resistance to wear, low thermal expansion, medium thermal conductivity, and good chemical resistance. This combination of properties makes silicon nitride ceramics appropriate for fabricating components subject to very high dynamic stresses and reliability requirements. Important fields of application include cutting tools, roller bearings, highly stressed machine elements, kiln furniture, melting crucibles, and ingot moulds used, for instance, in the manufacture of silicon components for solar technology.

Due to its great potential for use in structural applications, the mechanical behaviour of silicon nitride and related materials has been thoroughly characterized. However, this intensive mechanical characterization has been limited to either room temperature[4–6] or high temperatures within the creep regime.[7–10] The information available at intermediate temperatures is still very scarce — indeed limited to elastic property evaluations by dynamic measurements[11–16] — despite the fact that it is within this temperature range where silicon nitride has to work in most practical applications.

The primary objective of the present paper is to evaluate the suitability of a commercial silicon nitride available in the form

* Corresponding author.
*E-mail address:* estibalizsg@unex.es (E. Sánchez-González).

0955-2219/$ – see front matter © 2009 Elsevier Ltd. All rights reserved.
doi:10.1016/j.jeurceramsoc.2009.03.011

of precision spheres as indenter for the proposed mechanical characterization method above room temperature. For that purpose we will apply the same procedure used for the studies on alumina[3] and zirconia[2] to this silicon nitride. Consequently, this study will also serve to redress the aforementioned deficiency in the literature data by analyzing the effect of temperature on the mechanical behaviour of a silicon nitride under contact stresses from room temperature up to 1000 °C.

Typical indentation stress–strain curves are obtained from the Hertzian tests, and Young's modulus, $E$, is calculated from the slope of the linear part of the curves using Hertzian elastic theory. The yield stress, $Y$, and strain-hardening parameter, $n$, are evaluated by fitting FEM results to the experimental curves. The contact damage generated and the critical loads for crack initiation as a function of temperature are determined from observations of the indentation surface after the tests by optical microscopy. The results of this study and their implication for the practical use of silicon nitride as indenter in this temperature range are discussed. In particular, the advantages of silicon nitride over other conventional advanced ceramics in this temperature region are discussed by comparing these results with data from previous studies.[2,3]

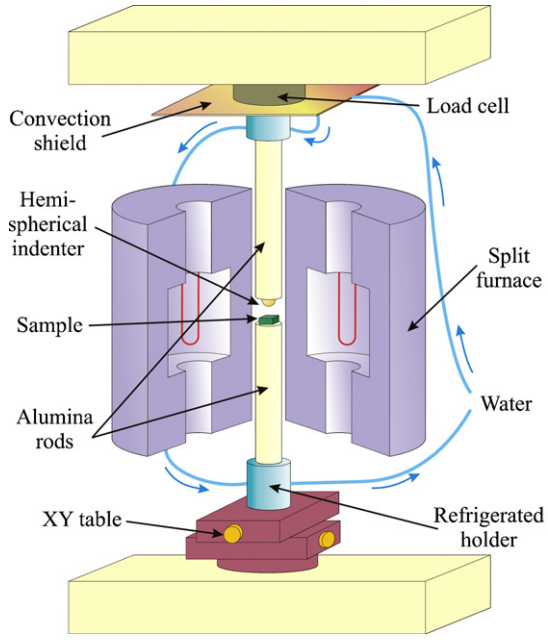


Fig. 1. Diagram of the experimental setup used for the Hertzian tests at intermediate temperatures.

## 2. Materials and experimental methods

### 2.1. Materials and microstructural characterization

The material chosen for this study was a commercial polycrystalline silicon nitride supplied by Marteau & Lemarié (Pantin, France) in the form of dense spheres of 3 and 9 mm radius. The smaller spheres were cut in half to be used as indenters, while disc specimens with a thickness of 8 mm were cut from the central regions of the larger spheres. This procedure ensured that specimen and indenter were alike materials. The test surfaces of the flat specimens were polished to 1 μm finish.

The microstructure morphology of this commercial silicon nitride was analyzed using conventional scanning electron microscopy (VP-SEM S-3600N, Hitachi Ltd., Japan) on induced fracture surfaces. The phase composition of the material was determined by Rietveld analysis from X-ray diffraction data (PW-1800, Philips, Holland) obtained using Cu Kα radiation (40 kV, 35 mA).

### 2.2. Mechanical testing

Hertzian contact tests were performed using a universal testing machine (AG-IS 100 kN, Shimadzu Corp., Kyoto, Japan) with an attached vertical split furnace, as schematized in Fig. 1. The furnace consisted of a cylindrical chamber with frontal aperture to facilitate access to indenter and specimen. The half-sphere indenter and the specimen were respectively bonded to the upper and lower alumina push rods (40 mm diameter and 350 mm length) using alumina paste (Ceramabond 569, Aremco Products Inc., New York, USA). External push rod holders were cooled with circulating water and a refrigerated convection shield was attached to the top holder to protect the load cell. The bottom push rod holder was placed on an $X$–$Y$ table that allowed multiple tests (more than 15) to be made on each specimen at any selected temperature. The surface of each specimen was sputter-coated (Polaron SC7640, East Sussex, UK) before the tests with a thin metallic film: Au, Rh–Pd, or Pt, depending on the testing temperature.[1] This procedure enables a clear residual impression of the contact area at peak load to be produced in the film even under elastic conditions.

Indentation sequences were performed in air at peak loads up to 10 000 N with a constant crosshead speed of 0.05 mm/min. Test temperatures were increased in 200 °C intervals up to the point at which creep effects on the size of the residual impression were noticeable. For this purpose, two 1000 N indentations were generated at each temperature, using two different crosshead speeds (0.05 and 0.005 mm/min). Since at 1200 °C the contact radius of the imprint at 0.005 mm/min was more than 10 μm larger than that at 0.05 mm/min, all the data from this temperature upwards were discarded. The system was heated at a rate of 6 °C/min, held for 1 h at the testing temperature before the indentations and then, after the tests, allowed to cool over several hours by switching off the furnace.

Plots of indentation stress ($p_0 = P/\pi a^2$) versus indentation strain ($a/r$) for each temperature were obtained from measurements of contact radius, $a$, obtained by optical microscopy from the corresponding residual impressions after cooling, for each peak load, $P$, and indenter radius, $r$. Note that these indentation stress–strain curves are independent of the indenter radius.[17,18] Young's modulus, $E$, at each prescribed temperature was determined from the linear region of the indentation stress–strain curve using the Hertzian relation for elastic contacts[18,19]:

$$p_0 = \frac{4/3\pi}{(1-\nu^2)/E + (1-\nu'^2)/E'}\frac{a}{r}, \quad p_0 < 1.1Y \tag{1}$$

where $\nu$ is Poisson's ratio, $Y$ is the yield stress, and the primes indicate indenter properties. When indenter and specimen are made of the same material Eq. (1) becomes:

$$p_0 = \frac{2E}{3\pi(1-\nu^2)}\frac{a}{r}, \quad p_0 < 1.1Y \tag{2}$$

In our case Poisson's ratio is assumed to be 0.24.

The surface damage — permanent quasi-plastic deformation, cone and/or radial cracks[18] — was observed by optical microscopy using Nomarsky contrast, and the critical loads for crack initiation were determined as the lowest applied load at which cracking was observed. The difference between this load and that immediately lower was used as the error for the critical load estimation. It is worth noting that ring/cone cracking modifies only the near-contact stress field and therefore does not affect the capacity of the material to sustain loads.[20] Indeed, cone cracking does not produce any observable load drop during tests. Consequently, neither does it affect the indentation stress–strain curves — for example, indentation stress–strain curves in soda-lime glass are perfectly linear[21] despite the cone cracks that develop at low loads in this material.

Critical loads for quasi-plastic damage initiation, $P_Y$, and their corresponding errors, were calculated from the expression[18,19]

$$P_Y = \frac{9}{16}\left(\frac{1-\nu^2}{E} + \frac{1-\nu'^2}{E'}\right)^2 (\pi p_Y)^3 r^2 \tag{3}$$

where $p_Y$ is the contact pressure at which either the specimen or the indenter starts to yield. For like materials, and taking into account that $p_Y \approx 1.1Y$,[18] this expression becomes:

$$P_Y = \frac{9(1-\nu^2)^2(1.1\pi Y)^3}{4E^2} r^2 \tag{4}$$

where $Y$ is yield stress of the material, whose values can be calculated from FEM as described below.

### 2.3. Finite element modeling

ABAQUS/Standard (SIMULIA, Providence, RI) FEM software was used to estimate the yield parameters of silicon nitride at each temperature. The algorithm models a deformable silicon nitride half-sphere of 3 mm radius in axisymmetric contact with a silicon nitride flat specimen of 15 mm thickness and 15 mm radius. These dimensions have been used in previous studies, and are large enough compared to the contact radii to avoid any free surface effect, as is the actual sample size (8 mm × 9 mm), therefore the stress field would be unaffected by these size differences between sample and model. The load applied to the half-sphere is incrementally increased up to a maximum of 10 000 N. The specimen and sphere grids consist of a total of more than 20 000 linear axisymmetric quadrilateral elements with reduced integration. Element dimensions range from a minimum of 1 μm × 1 μm around the contact region to hundreds of microns in regions far from the contact. The following constitutive uniaxial elasto-plastic model[1] is assumed in the calculations:

$$\begin{aligned} \sigma &= E\varepsilon, \quad (\sigma < Y) \\ \sigma &= \left[\left(\frac{E}{Y}\right)^n Y\right]\varepsilon^n \quad (\sigma > Y) \end{aligned} \tag{3}$$

where $n$ is the dimensionless strain-hardening coefficient, with value between 0 (fully plastic) and 1 (fully elastic). These constitutive equations are based on a critical shear condition for yield but incorporating a strain-hardening characteristic to allow for local elastic constraints on the sliding shear faults that are responsible for quasi-plasticity in ceramic materials.[6,18,22–24] These uniaxial equations are then generalized to multiaxial behavior using the von Mises yield criterion. The application of this type of treatment, typically used in metallic materials, to quasi-plastic ceramics has been justified by Fischer-Cripps and Lawn,[25,26] and proved to be useful for predicting the main features of Hertzian stress–strain curves and the evolving deformation zone geometries, despite the fact that the underlying deformation mechanism is shear faulting instead of dislocation sliding. The model used here is just a modification of the simple bilinear model used by those authors[21,27–29] so as to consider a more realistic, non-linear, strain-hardening behavior. For each temperature the values of $Y$ and $n$ are iteratively adjusted by trial and error to fit the FEM calculated indentation stress–strain curve to the experimental data, using the values of $E$ — determined as described in the previous section — and $\nu$ as input parameters. It must be stressed that the proposed FE constitutive model does not pretend to reproduce all the complex mechanisms that may be involved in quasi-plastic deformation (shear fault sliding, microcracking, twinning, etc.). It is just used as a simple means to estimate two mechanical parameters ($Y$ and $n$) in order to be able to more quantitatively compare the deviations from linear behaviour of different ceramic materials under contact stresses.

## 3. Results and discussion

Fig. 2 shows an SEM micrograph of a fracture surface in the commercial silicon nitride. As can be appreciated, the material

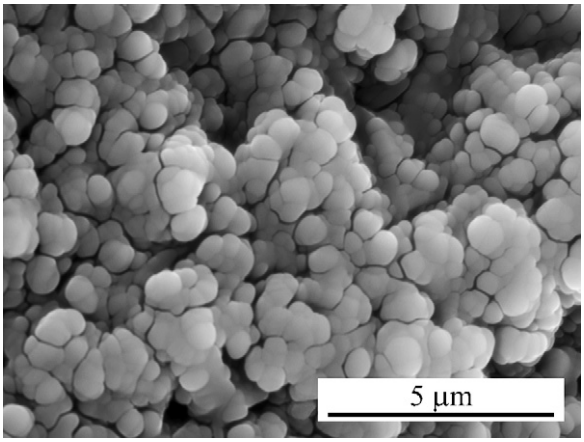


Fig. 2. SEM micrograph of a fracture surface of the polycrystalline silicon nitride studied in this work.

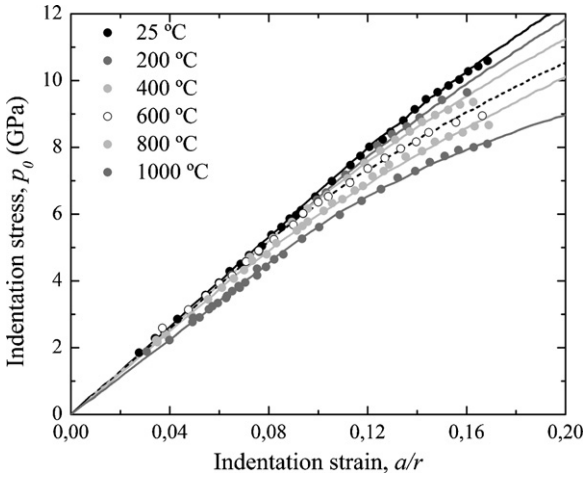


Fig. 3. Indentation stress–strain data for polycrystalline silicon nitride at designated temperatures. Hertzian tests were performed with like-material indenters of 3 mm radius and peak loads up to 10 000 N. Solid curves through experimental data are FEM best fits.

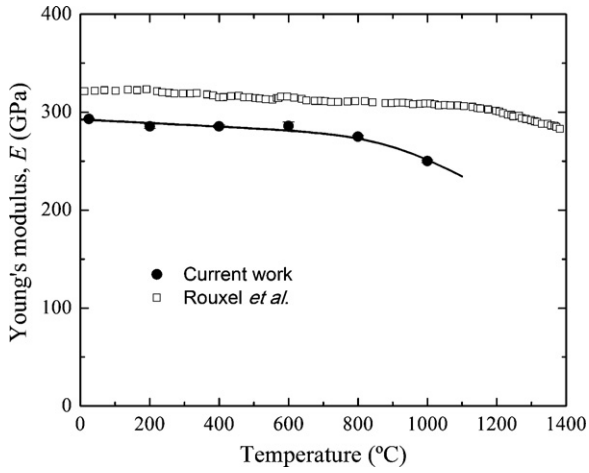


Fig. 4. Plot of Young's modulus versus temperature for polycrystalline silicon nitride. The data points were obtained from the slope of the linear part of the stress–strain curves of Fig. 3 and Eq. (2). Error bars are smaller than symbols and the solid line is an empirical fit. Data from Bruls et al. are also included in the figure for comparison.[30]

has a very homogeneous microstructure, with an average grain size smaller than 1 μm. The Rietveld analysis of the X-ray diffraction data showed that the silicon nitride was largely in its β phase (92.3 ± 0.6 wt%), with a minor amount of α phase (7.7 ± 0.6 wt%).

Indentation stress–strain curves for this material at temperatures ranging from 25 °C to 000 °C are shown in Fig. 3. Each point in these curves represents a single indentation performed at a prescribed peak load. The solid lines through the experimental data are FEM best-fits obtained as described in the previous section. For each temperature, the initial part of the corresponding curve is linear and, at a certain indentation stress ($p_Y \approx 1.1Y$), the data depart from linearity indicating the onset of quasi-plastic yield. Comparison of these curves clearly shows a slight decrease in both the slope of the linear part and the yield stress with temperature, which becomes more noticeable at the higher temperatures.

Young's moduli calculated from the best-fit slopes to the linear regions of the stress–strain curves using Eq. (2) are plotted versus temperature in Fig. 4. The standard deviations of the data have been included as error bars but are smaller than the symbol size in all cases. The solid line through the data points is an empirical fit. The elastic modulus exhibits a slow linear decrease (18 MPa/°C) with increasing temperature up to approximately 800 °C, and then the rate of decrease becomes faster. Similar Youngĭs modulus dependences on temperature have been reported in the literature for this and other materials, and the transition is always attributed to the activation of reversible grain boundary sliding[1,11,30] — a set of data for $Si_3N_4$ from the literature which were obtained by the impulse excitation technique has been included in Fig. 4 for comparison. The transition temperature from slow to fast modulus degradation in $Si_3N_4$ has been shown to depend on the amount and type of sintering additives used for its processing.[16] Additives deposit at the grain boundaries, determining their strength, which is obviously related to the temperature for the activation of the sliding.

The yield stress for this $Si_3N_4$, determined from FEM as described in the previous section, is shown in Fig. 5 as a function of temperature. The error bars indicate the estimated maximum uncertainties and the solid line through the data is an empirical fit. The yield stress decreases with increasing temperature up to about 800 °C and then levels off. Such a plateau indicates that, beyond this temperature, thermal energy cannot further assist the initiation of the intragranular shear faults that are responsible for quasi-plastic deformation in this material.[6,22] The strain-hardening parameter obtained from FEM, however, was found to be constant, within the uncertainties, over the whole temperature range ($n = 0.3 \pm 0.1$), indicating a certain strain-hardening capability in this material that is not degraded by increasing temperature.

Fig. 6 shows micrographs of the surface damage induced with a 3 mm indenter radius and 2200 N load at room tem-

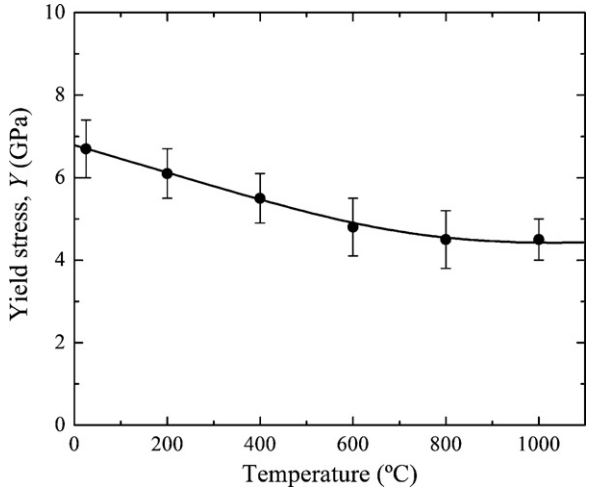


Fig. 5. Plot of yield stress versus temperature for polycrystalline silicon nitride. Each datum was estimated through a fit to the indentation stress–strain data using the FEM algorithm. The error bars indicate the estimated maximum uncertainties in these estimates, and the solid line through the data is an empirical fit.

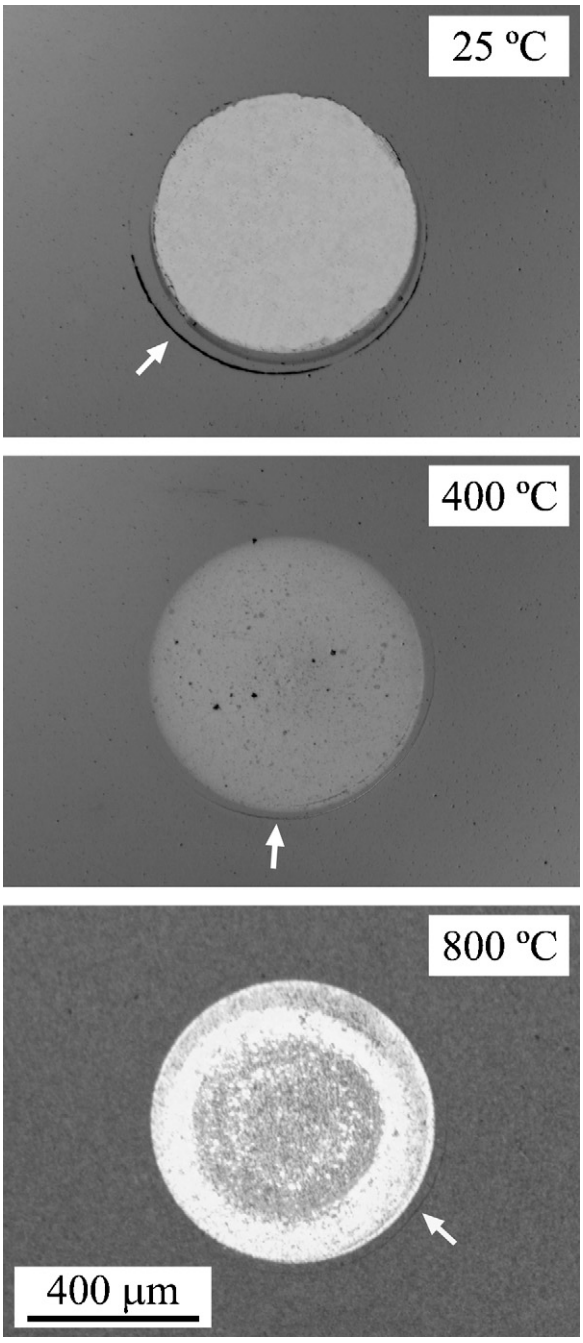


Fig. 6. Optical micrographs showing surface Hertzian damage in polycrystalline silicon nitride generated with a like-material indenter of 3 mm radius at 2200 N peak load for (a) room temperature, (b) 400 °C, and (c) 800 °C. Arrows indicate ring/cone cracks.

perature, 400 °C and 800 °C. Ring/cone cracks (white arrows) are apparent in all the micrographs, and it can be appreciated that the residual impression increases slightly with temperature due to the reduction of the elastic modulus and yield stress (see Figs. 4 and 5). Permanent deformations, though not clearly noticeable in the figure, were evidenced at 400 °C and 800 °C by Nomarsky illumination as a slight depression in the test surface. Radial cracks — which, in monolithic materials under contact stresses, appear due to coalescence of microcracks associated with quasi-plastic damage[31] — were never observed at any of

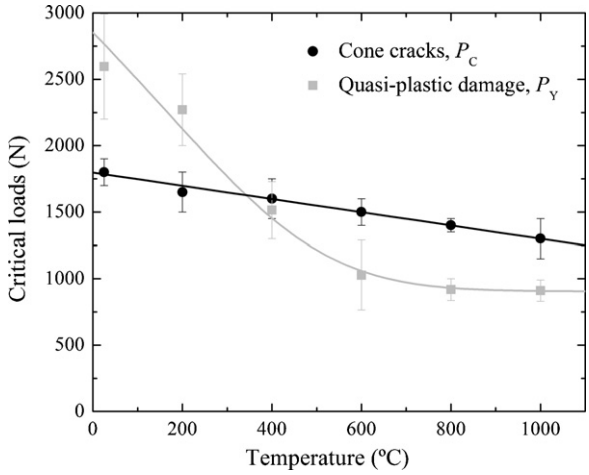


Fig. 7. Critical loads for the initiation of quasi-plastic damage, $P_Y$, and cone cracking, $P_C$, in silicon nitride as a function of temperature. The data and error bars were determined as described in the experimental section, and the solid lines are empirical fits.

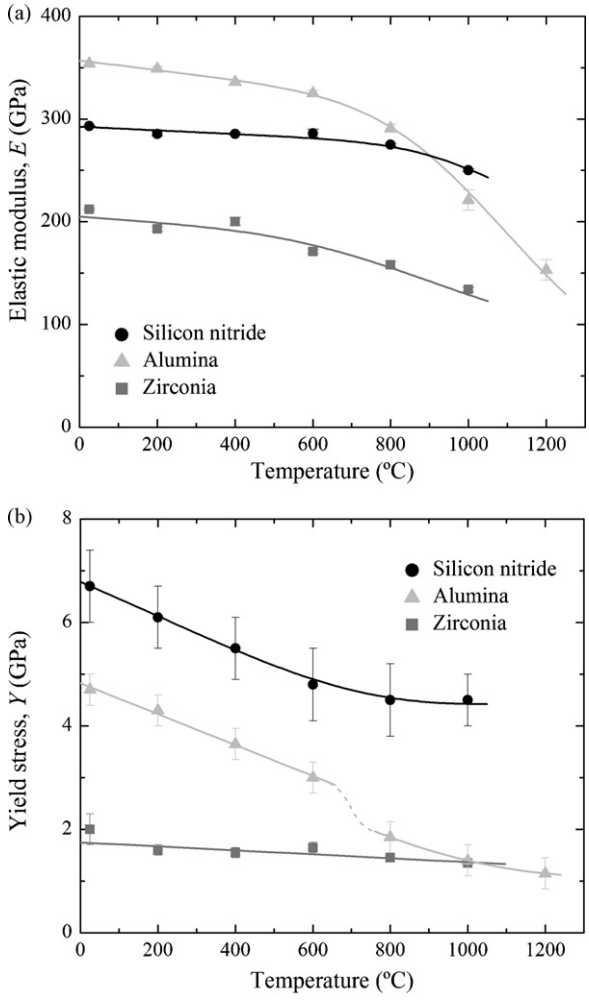


Fig. 8. Comparison of the evolution with temperature of (a) the elastic moduli and (b) the yield stresses of silicon nitride, with data for alumina[3] and zirconia,[2] from previous work. The error bars indicate the estimated uncertainties and the solid lines through the data are empirical fits.

the temperatures. This indicates that either shear faults responsible for quasi-plastic deformation do not generate microcracks or that the applied loads (up to 10 000 N) are insufficient for microcracks to coalesce into macroscopic cracks. This indicates that the amount of quasi-plastic damage generated during the tests was moderate, and suggests that this material exhibits significant contact damage resistance over the whole temperature range.

Fig. 7 shows the critical loads for the initiation of quasi-plastic damage, $P_Y$, calculated from Eq. (4), and cone cracking, $P_C$, as a function of temperature. The data and error bars in this plot were determined as described in the preceding section, and the solid lines are empirical fits to the experimental data. Both magnitudes decline with temperature due to the increase in the thermal energy available for the initiation of both types of damage modes. This plot allows one to analyze which is the primary damage mode in this material at each temperature—quasi-plastic damage or cone cracks. As can be clearly appreciated, this silicon nitride exhibits a brittle-to-ductile transition at around 400 °C. At lower temperatures cone cracking is the first damage mode, but $P_C$ decreases linearly and relatively slowly ($0.5 \pm 0.1$ N/°C) with increasing temperature while $P_Y$ falls off faster (~3 N/°C), and thus quasi-plasticity becomes the first damage mode above 400 °C, in spite of $P_Y$ reaching a plateau.

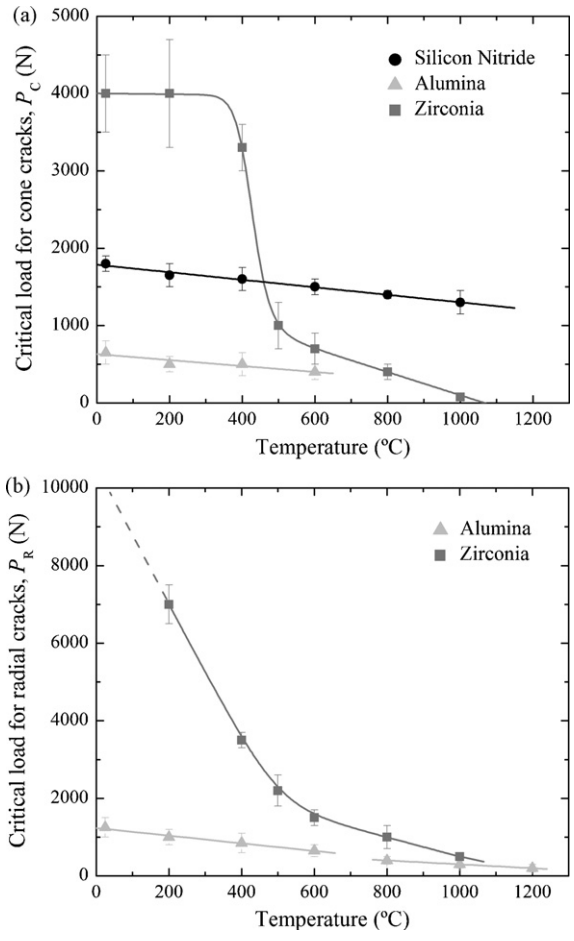


Fig. 9. Comparison of the evolution with temperature of critical loads for initiation of (a) ring/cone and (b) radial cracks on silicon nitride, with data for alumina[3] and zirconia,[2] from previous work. The error bars indicate the estimated uncertainties and the solid lines through the data are empirical fits. Note that no radial cracks were observed in silicon nitride within the load range applied (up to 10 000 N).

### 3.1. Comparison with other commercial materials

Fig. 8 shows a comparison of the evolution with temperature of the elastic moduli (Fig. 8a) and yield stresses (Fig. 8b) of silicon nitride and two other commercial materials, alumina and zirconia, analyzed in previous work using the same approach.[2,3] According to these results, alumina is the stiffest material up to 800 °C but its modulus degrades rather quickly with increasing temperature, and it is surpassed by silicon nitride above that temperature. Indeed, the elastic modulus of silicon nitride exhibits the mildest degradation over the temperature range analyzed. Although not so stable with temperature, the yield stress of silicon nitride is significantly higher than for the other two materials, and its degradation with temperature does not continue above 800 °C. Besides, as shown in Fig. 9, the critical loads for cone (Fig. 9a) and radial (Fig. 9b) cracking in $Si_3N_4$ are higher than for the other two materials — indeed, no radial cracks were observed in $Si_3N_4$ up to 10 000 N — with the only exception of cone cracking in zirconia below 500 °C due to the activation of the transformation toughening mechanism.[2]

## 4. Conclusions

In this work, we have used a recently developed method, combining Hertzian indentation and FEM simulation, to study the elasto-plastic behaviour and contact damage evolution of a commercial polycrystalline silicon nitride from room temperature to 1000 °C. Although the direct measurements performed in this study were made on flat specimens rather than on the sphere for practical reasons, it is evident that all the results are equally applicable to the indenter, as they are made of the same material. The great stiffness and yield stress exhibited by silicon nitride, and its resistance to contact damage, make this material a particularly good standard choice for the spherical indenters used to evaluate the mechanical properties at elevated temperature of other materials following the procedure applied in this work. Therefore, the relevance of this study is that it provides the indenter parameters required for deconvoluting the mechanical properties of any tested material at each temperature. The indenter's Young's modulus is needed to calculate the modulus and the critical load for yield from Eqs. (1) and (3), respectively, while the set of indenter properties ($E'$, $Y'$, $n'$) are used as input parameters in the FEM simulations needed to obtain the yield stress and the work-hardening parameter of the tested material. The characterization of the indenter material provided here thus standardizes the proposed method, which can now be applied to investigating the mechanical properties of any hard material of interest up to its creep temperature or that of $Si_3N_4$, whichever is lower.

## Acknowledgements

This work was funded by the Ministerio de Ciencia y Tecnología (Government of Spain) and the Fondo Social Europeo through grant MAT2006-08720.

## References


1. Sanchez-Gonzalez, E., Melendez-Martinez, J. J., Pajares, A., Miranda, P., Guiberteau, F. and Lawn, B. R., Application of Hertzian tests to measure stressstrain characteristics of ceramics at elevated temperatures. *J. Am. Ceram. Soc.*, 2007, **90**, 149–153.
2. Sanchez-Gonzalez, E., Miranda, P., Melendez-Martinez, J. J., Guiberteau, F. and Pajares, A., Contact properties of yttria partially stabilized zirconia up to 1000 degrees C. *J. Am. Ceram. Soc.*, 2007, **90**, 3572–3577.
3. Sanchez-Gonzalez, E., Miranda, P., Melendez-Martinez, J. J., Guiberteau, F. and Pajares, A., Temperature dependence of mechanical properties of alumina up to the onset of creep. *J. Eur. Ceram. Soc.*, 2007, **27**, 3345–3349.
4. De Arellano-Lopez, A. R., Mcmann, M. A., Singh, J. P. and Martinez-Fernandez, J., Microstructure and room-temperature mechanical properties of $SI_3N_4$ with various alpha/beta phase ratios. *J. Mater. Sci.*, 1998, **33**, 5803–5810.
5. Lee, S. K. and Lawn, B. R., Contact fatigue in silicon nitride. *J. Am. Ceram. Soc.*, 1999, **82**, 1281–1288.
6. Lee, S. K., Wuttiphan, S. and Lawn, B. R., Role of microstructure in Hertzian contact damage in silicon nitride. 1. Mechanical characterization. *J. Am. Ceram. Soc.*, 1997, **80**, 2367–2381.
7. Melendez-Martinez, J. J. and Dominguez-Rodriguez, A., Creep of silicon nitride. *Prog. Mater. Sci.*, 2004, **49**, 19–107.
8. Melendez-Martinez, J. J., Gomez-Garcia, D., Jimenez-Melendo, M. and Domiguez-Rodriguez, A., Creep mechanism of gas-pressure-sintered silicon nitride polycrystals—I. Macroscopic and microscopic experimental study. *Philos. Mag.*, 2004, **84**, 3375–3386.
9. Melendez-Martinez, J. J., Gomez-Garcia, D., Jimenez-Melendo, M. and Domiguez-Rodriguez, A., Creep mechanism of gas-pressure-sintered silicon nitride polycrystals—II. Deformation mechanism. *Philos. Mag.*, 2004, **84**, 3387–3395.
10. Melendez-Martinez, J. J., Jimenez-Melendo, M., Dominguez-Rodriguez, A. and Wotting, G., Creep behaviour of two sintered silicon nitride ceramics. *J. Eur. Ceram. Soc.*, 2002, **22**, 2495–2499.
11. Roebben, G., Duan, R. G., Sciti, D. and Van der Biest, O., Assessment of the high temperature elastic and damping properties of silicon nitrides and carbides with the impulse excitation technique. *J. Eur. Ceram. Soc.*, 2002, **22**, 2501–2509.
12. Roebben, G., Donzel, L., Steen, M., Schaller, R. and Van der Biest, O., Fatigue resistant silicon nitride ceramics due to anelastic deformation and energy dissipation. *J. Alloys Compd.*, 2000, **310**, 39–43.
13. Roebben, G., Basu, B., Vleugels, J., Van Humbeeck, J. and Van der Biest, O., The innovative impulse excitation technique for high-temperature mechanical spectroscopy. *J. Alloys Compd.*, 2000, **310**, 284–287.
14. Roebben, G. and Van der Biest, O., *Elastic and Anelastic Properties of Silicon Nitride at High Temperatures by Non-destructive Impulse Excitation*. Trans Tech Publications Ltd., Zurich-Uetikon, 2000.
15. Tomeno, I., High-temperature elastic-moduli of $SI_3N_4$ ceramics. *Jpn. J. Appl. Phys.*, 1981, **20**, 1751–1752.
16. Rouxel, T., Sangleboeuf, J. C., Huger, M., Gault, C., Besson, J. L. and Testu, S., Temperature dependence of Young's modulus in $SI_3N_4$-based ceramics: roles of sintering additives and of SiC-particle content. *Acta Mater.*, 2002, **50**, 1669–1682.
17. Tabor, D., *The Hardness of Metals*. Oxford University Press, London, UK, 1951.
18. Lawn, B. R., Indentation of ceramics with spheres: a century after Hertz. *J. Am. Ceram. Soc.*, 1998, **81**, 1977–1994.
19. Johnson, K. L., *Contact Mechanics*. Cambridge Univ. Press, Cambridge, UK, 1985.
20. Frank, F. C. and Lawn, B. R., On theory of Hertzian fracture. *Proc. R. Soc. Lond. Ser. A-Math. Phys. Sci.*, 1967, **299**, 291–306.
21. Miranda, P., Pajares, A., Guiberteau, F., Cumbrera, F. L. and Lawn, B. R., Contact fracture of brittle bilayer coatings on soft substrates. *J. Mater. Res.*, 2001, **16**, 115–126.
22. Xu, K. H. K., Wei, L. H., Padture, N. P., Lawn, B. R. and Yeckley, R. L., Effect of microstructural coarsening on Hertzian contact damage in silicon-nitride. *J. Mater. Sci.*, 1995, **30**, 869–878.
23. Lawn, B. R., Padture, N. P., Cai, H. D. and Guiberteau, F., Making ceramics ductile. *Science*, 1994, **263**, 1114–1116.
24. Guiberteau, F., Padture, N. P., Cai, H. and Lawn, B. R., Indentation fatigue—a simple cyclic Hertzian test for measuring damage accumulation in polycrystalline ceramics. *Philos. Mag. A-Phys. Condens. Matter Struct. Defect Mech. Prop.*, 1993, **68**, 1003–1016.
25. Fischer-Cripps, A. C. and Lawn, B. R., Indentation stress–strain curves for "quasiductile" ceramics. *Acta Mater.*, 1996, **44**, 519–527.
26. Fischer-Cripps, A. C. and Lawn, B. R., Stress analysis of contact deformation in quasi-plastic ceramics. *J. Am. Ceram. Soc.*, 1996, **79**, 2609–2618.
27. Zhao, H., Miranda, P., Lawn, B. R. and Hu, X. Z., Cracking in ceramic/metal/polymer trilayer systems. *J. Mater. Res.*, 2002, **17**, 1102–1111.
28. Miranda, P., Pajares, A., Guiberteau, F., Deng, Y. and Lawn, B. R., Designing damage-resistant brittle-coating structures: I. Bilayers. *Acta Mater.*, 2003, **51**, 4347–4356.
29. Miranda, P., Pajares, A., Guiberteau, F., Deng, Y., Zhao, H. and Lawn, B. R., Designing damage-resistant brittle-coating structures: II. Trilayers. *Acta Mater.*, 2003, **51**, 4357–4365.
30. Bruls, R. J., Hintzen, H. T., de With, G. and Metselaar, R., The temperature dependence of the Young's modulus of $MgSiN_2$, AlN and $Si_3N_4$. *J. Eur. Ceram. Soc.*, 2001, **21**, 263–268.
31. Cai, H. D., Kalceff, M. A. S. and Lawn, B. R., Deformation and fracture of mica-containing glass–ceramics in Hertzian contacts. *J. Mater. Res.*, 1994, **9**, 762–770.